International Journal of Non-Linear Mechanics 53 (2013) 75–82

Contents lists available at SciVerse ScienceDirect

International Journal of Non-Linear Mechanics

journal homepage: www.elsevier.com/locate/nlm

Model reduction for efficient time-integration of planar flexible multibody models

S.E. Boer [a,*], D. ten Hoopen [a], R.G.K.M. Aarts [a], W.B.J. Hakvoort [a,b], J.B. Jonker [a]

[a] Faculty of Engineering Technology, University of Twente, P.O. Box 217, 7500 AE, Enschede, The Netherlands
[b] Demcon Advanced Mechatronics, Zutphenstraat 25, 7575 EJ, Oldenzaal, The Netherlands

ARTICLE INFO

Available online 24 January 2013

Keywords:
Non-linear model reduction
Modal basis
Singular value decomposition
Geometric non-linearity
Compliant mechanism

ABSTRACT

A reduction method is proposed for efficient time-integration of (planar) compliant mechanism models that undergo large deflections. Models for this class of mechanisms have to include an accurate description of geometric non-linearities, as stiffness characteristics can change significantly during deflection. A finite element based flexible multibody approach is used to analyse compliant mechanisms in terms of independent coordinates. Geometric transfer functions are applied to express the configuration and deformed state in terms of the independent coordinates. The modelling of large deflections requires using a sufficient number of finite elements to ensure that deformations remain small in a co-rotational context. Increasing the number of elements, increases, besides the number of degrees of freedom, the largest eigenfrequency in the model. This reduces the allowable step size in explicit time-integrator methods.

For the proposed reduction method, we aim to suppress the unwanted high frequency modes to increase the allowable step size. This is accomplished by first choosing, where possible, coordinates that remain small during simulation as independent coordinates. Such coordinates are well suited to be reduced using linear projection methods such as modal projection for suppressing the high frequency modes. The configuration and deformed state of the mechanism is subsequently determined with the geometric transfer functions. Consequently, a significant increase in the allowable step size is realised, while retaining the geometric non-linear effects that are contained in the geometric transfer functions.

The effectiveness of the method is demonstrated by two planar examples: a compliant straight guidance that undergoes large deflections and a flexible manipulator.

1. Introduction

Compliant mechanisms equipped with flexure based hinges are often utilised in high precision manipulator devices for their deterministic static and dynamic behaviour. The analysis for design and control of compliant mechanisms undergoing large deflections relies on computational efficient models that are capable of capturing the relevant dynamic and compliant characteristics over the full range of motion. These models should offer a sound inclusion of geometric non-linear effects.

In [1] we discuss a modelling approach for the analysis and simulation of multibody systems with flexible components where a multibody system is modelled as the assembly of non-linear finite elements. For each element a fixed number of deformation modes are defined with associated deformation coordinates that are invariant for arbitrary rigid body motion. Typical flexible members of compliant mechanisms are wire and sheets flexures. These flexures may be considered as one-dimensional structures which can be correctly modelled by flexible beam elements. Though, a rather large number of flexible beam elements may be needed to obtain a model that correctly captures the geometric non-linear effects for large deformations. Consequently, high frequency modes are introduced in the model that greatly deteriorate the computational efficiency, in particular if explicit integrators are used for the time-integration of the non-linear equations of motion.

For linear mechanical systems, these higher frequency modes can be removed using model reduction techniques that project the dynamics onto a lower dimensional subspace while preserving the dominant dynamical behaviour. Research on model reduction techniques applied to non-linear flexible multibody systems can be separated into two categories: component and system level model reduction. System level model reduction generally has a large impact on the computational time of simulations, whereas component level reduction techniques are employed for the efficient modelling of complex-shaped

* Corresponding author. Tel.: +31 53 489 2502.
E-mail address: S.E.Boer@utwente.nl (S.E. Boer).

0020-7462/$ - see front matter © 2013 Elsevier Ltd. All rights reserved.
http://dx.doi.org/10.1016/j.ijnonlinmec.2013.01.009

components [2–5]. The adaptive modal integration (AMI) method introduced by Aarts and Jonker [6] and the global modal parameterisation (GMP) method introduced by Brüls et al. [7] are examples of system level model reduction techniques. Both methods separate the motion of the mechanism in a non-linear nominal rigid body motion and a configuration dependent elastic motion part. The AMI method is applied to a set of non-linear equations of motion expressed as ordinary differential equations (ODE) for a set of independent coordinates, as in [1]. Using locally linearised models, a set of linear time-varying ODE's is obtained for the elastic motion. With modal reduction techniques, the order of these equations is reduced. The GMP method is applied to a general set of differential algebraic equations (DAE). By combining linearised models with the constraint equations and applying modal reduction techniques, also a cheaper to solve set of ODE's is obtained for the elastic motion. Both methods in their current approach assume that the elastic deformations remain small with respect to the rigid body motion, making them less suited to reduce models describing compliant mechanisms that undergo large deflections.

For this reason, we aim to reduce the non-linear equations of motion of a multibody system with flexible components expressed as ODE's for a set of independent coordinates [1]. This approach has been implemented in the SPACAR software [8]. Geometric transfer functions are used to express the configuration and deformation state of the mechanism as explicit functions of these independent coordinates. In the proposed reduction method, the number of independent coordinates is reduced by imposing linear relations between them. To that end independent coordinates are selected which remain small during simulation and therefore are suitable to be reduced using linear projection methods. The reduction of independent coordinates effectively suppresses the excitation of high frequency modes while the dominant geometric non-linear effects are retained in the geometric transfer functions. This makes the approach suitable for reduction of compliant mechanisms undergoing large deflections.

The effectiveness of the method is demonstrated with two planar examples: a compliant straight guidance that undergoes large deflections and a flexible manipulator. The applicability of the reduction method is shown for these classes of planar mechanisms, whereas spatial systems are addressed elsewhere [9].

2. Finite element modelling

A brief introduction is given on the finite element representation used to model the compliant mechanism and flexible manipulator considered in this paper. Then, using the concept of geometric transfer functions, we derive the equations of motion in terms of independent generalised coordinates. Finally, the linearised equations of motion are presented which are used for modal analyses in Section 3.

2.1. Finite element representation

In the presented finite element method, a compliant mechanism or a flexible manipulator is modelled as an assembly of finite elements interconnected by joint elements which can be hinge elements or a subassembly of flexible beam elements that represent a flexible joint. The location of each element is described relative to a fixed inertial coordinate system by a set of nodal coordinates $\boldsymbol{x}^{(k)}$, valid for large displacements and rotations. Some coordinates are Cartesian coordinates of the end nodes, while others describe the orientation of orthogonal base vectors or triads, rigidly attached to the element nodes. The superscript k indicates that a specific element k is considered. With respect to some reference configuration of the element, the instantaneous values of the nodal coordinates represent a fixed number of deformation modes for the element. The deformation modes are specified by a set of deformation coordinates $\boldsymbol{\epsilon}^{(k)}$ that are invariant for arbitrary motion of the element as a rigid body. Hence, the number of deformation coordinates is equal to the number of nodal coordinates minus the number of degrees of freedom of the element as a rigid body. The components of the vector of deformation coordinates $\boldsymbol{\epsilon}^{(k)}$ can be expressed as analytical functions of the vector of nodal coordinates $\boldsymbol{x}^{(k)}$. In this way we can define for each element k a vector function

$$\boldsymbol{\epsilon}^{(k)} = \boldsymbol{\mathcal{D}}^{(k)}(\boldsymbol{x}^{(k)}). \tag{1}$$

As a first example, the deformation functions $\mathcal{D}_i^{(k)}$ of the planar beam element are presented. As nodal coordinates we have four Cartesian coordinates (x^p, y^p), (x^q, y^q) describing the nodal positions of the beam element in the inertial reference frame and two rotation angles φ^p and φ^q that describe the orientations of the nodes with respect to the initial undeformed orientation of the element given by the angle β_0. Hence the vector of nodal coordinates is then

$$\boldsymbol{x}_{\text{beam}}^{(k)} = \begin{bmatrix} \boldsymbol{r}^p \\ \varphi^p \\ \boldsymbol{r}^q \\ \varphi^q \end{bmatrix} = [x^p \;\; y^p \;\; \varphi^p \;\; | \;\; x^q \;\; y^q \;\; \varphi^q]^{\mathrm{T}}. \tag{2}$$

The number of degrees of freedom of the element as a rigid body is three, which gives rise to three deformation coordinates. The first deformation coordinate $\varepsilon_1^{(k)}$ represents the elongation of the element

$$\begin{aligned} \varepsilon_1^{(k)} &= \mathcal{D}_1^{(k)}(\boldsymbol{x}_{\text{beam}}^{(k)}) \\ &= l^{(k)} - l_0^{(k)} + \frac{1}{30 l_0^{(k)}}(2(\varepsilon_2^{(k)})^2 + \varepsilon_2^{(k)}\varepsilon_3^{(k)} + 2(\varepsilon_3^{(k)})^2), \end{aligned} \tag{3a}$$

where $l^{(k)} = \|\boldsymbol{r}^q - \boldsymbol{r}^p\|$ and $l_0^{(k)}$ is the reference length of the element. In addition two deformation coordinates $\varepsilon_2^{(k)}$ and $\varepsilon_3^{(k)}$, associated with the bending deformation of the beam element, can be defined [10]

$$\begin{aligned} \varepsilon_2^{(k)} &= \mathcal{D}_2^{(k)}(\boldsymbol{x}_{\text{beam}}^{(k)}) \\ &= \frac{l_0^{(k)}}{l^{(k)}}((x^q - x^p)\sin(\varphi^p + \beta_0) \\ &\quad -(y^q - y^p)\cos(\varphi^p + \beta_0)), \end{aligned} \tag{3b}$$

$$\begin{aligned} \varepsilon_3^{(k)} &= \mathcal{D}_3^{(k)}(\boldsymbol{x}_{\text{beam}}^{(k)}) \\ &= -\frac{l_0^{(k)}}{l^{(k)}}((x^q - x^p)\sin(\varphi^q + \beta_0) \\ &\quad -(y^q - y^p)\cos(\varphi^q + \beta_0)). \end{aligned} \tag{3c}$$

Note that in the expression for the elongation $\varepsilon_1^{(k)}$ second order geometric terms are included representing additional shortening of the beam axis caused by bending [11]. The deformation coordinates in Eq. (3) posses the proper invariance with respect to rigid body motions of the beam element.

The second example is the planar hinge element which can be used to describe the relative angle between two beam elements. The vector of nodal coordinates is

$$\boldsymbol{x}_{\text{hinge}}^{(k)} = [\varphi^p, \varphi^q]^{\mathrm{T}}, \tag{4}$$

where p and q are the nodes at both sides of the hinge. There is a single deformation coordinate, which is the relative rotation angle $\varepsilon_1^{(k)}$ defined as

$$\varepsilon_1^{(k)} = \mathcal{D}_1^{(k)}(\boldsymbol{x}_{\text{hinge}}^{(k)}) = \varphi^q - \varphi^p. \tag{5}$$

For a description of deformation functions of spatial beam and hinge elements the reader is referred to [9,12,10].

2.2. Equations of motion

A compliant mechanism or flexible manipulator can be built up with finite elements by letting them have nodal points in common. The assemblage of finite elements is realised by defining a vector $\boldsymbol{x}$ of nodal coordinates for the entire mechanism. The deformation functions of the elements can be described in terms of the components of the vector $\boldsymbol{x}$ yielding the non-linear vector function

$$\boldsymbol{\epsilon} = \mathcal{D}(\boldsymbol{x}), \tag{6}$$

which represents the basic equations for the kinematic analysis. Kinematic constraints can be introduced by putting conditions on the nodal coordinates $\boldsymbol{x}$ as well as by imposing conditions on the deformation coordinates $\boldsymbol{\epsilon}$ which are all assumed to be holonomic. For instance, rigidity of the elements can be enforced by imposing zero conditions on the subset of deformation coordinates associated with these elements, denoted by $\boldsymbol{\epsilon}^{(0)} = \mathcal{D}^{(0)}(\boldsymbol{x}) = \boldsymbol{0}$.

An important notion in the kinematic and dynamic analysis of mechanisms is that of degrees of freedom. The number of kinematic degrees of freedom is the smallest number of coordinates that describe, together with the kinematic constraints, the configuration of the mechanism. We call them independent generalised coordinates which are denoted by the superscript (m) and can be relative deformation coordinates, denoted by $\boldsymbol{\epsilon}^{(m)}$, or absolute nodal coordinates, denoted by $\boldsymbol{x}^{(m)}$. In this paper we choose to use only the deformation coordinates as independent generalised coordinates. The objective of kinematic analysis is then to solve Eq. (6) for the vector of independent generalised coordinates $\boldsymbol{q} = \boldsymbol{\epsilon}^{(m)}$. The solution is expressed by means of geometric transfer functions $\mathcal{F}$ and $\mathcal{E}$ as

$$\boldsymbol{x} = \mathcal{F}(\boldsymbol{q}), \quad \boldsymbol{\epsilon} = \mathcal{E}(\boldsymbol{q}). \tag{7}$$

The nodal velocities $\dot{\boldsymbol{x}}$ and accelerations $\ddot{\boldsymbol{x}}$ can be computed from (7) as

$$\dot{\boldsymbol{x}} = \frac{\partial \mathcal{F}}{\partial \boldsymbol{q}}\dot{\boldsymbol{q}} = \mathcal{F}_{,\boldsymbol{q}}\dot{\boldsymbol{q}}. \tag{8a}$$

$$\ddot{\boldsymbol{x}} = \left(\frac{\partial^2 \mathcal{F}}{\partial \boldsymbol{q}^2}\dot{\boldsymbol{q}}\right)\dot{\boldsymbol{q}} + \frac{\partial \mathcal{F}}{\partial \boldsymbol{q}}\ddot{\boldsymbol{q}} = (\mathcal{F}_{,\boldsymbol{qq}}\dot{\boldsymbol{q}})\dot{\boldsymbol{q}} + \mathcal{F}_{,\boldsymbol{q}}\ddot{\boldsymbol{q}}. \tag{8b}$$

Here the subscript notation "$,\boldsymbol{q}$" is used to denote partial differentiation with respect to the vector of independent coordinates $\boldsymbol{q}$. The geometric transfer functions $\mathcal{F}$ and $\mathcal{E}$ and their derivatives are determined numerically in an iterative way [12].

The inertia properties of the concentrated and distributed mass of the elements are described with the aid of configuration dependent lumped and consistent mass matrices [12]. Let $\boldsymbol{M}(\boldsymbol{x})$ be the global mass matrix, obtained by assembling the lumped and consistent element mass matrices, and let $\boldsymbol{f}(\boldsymbol{x},\dot{\boldsymbol{x}},t)$ be the vector of external nodal forces, including gravitational forces and the velocity dependent inertia forces. The loading state of each element is described by a vector of stress resultants. They are collected in the assembled vector $\boldsymbol{\sigma}$ which is dual to the vector of deformation coordinates $\boldsymbol{\epsilon}$. According to the principle of virtual work we obtain for the equations of motion of the mechanism

$$\delta\boldsymbol{x}^{\mathrm{T}}(\boldsymbol{f} - \boldsymbol{M}\ddot{\boldsymbol{x}}) = \delta\boldsymbol{\epsilon}^{\mathrm{T}}\boldsymbol{\sigma}, \tag{9}$$

for all virtual variations $\delta\boldsymbol{x}$ and $\delta\boldsymbol{\epsilon}$ which satisfy the instantaneous kinematic constraints

$$\delta\boldsymbol{x} = \mathcal{F}_{,\boldsymbol{q}}\delta\boldsymbol{q}, \quad \delta\boldsymbol{\epsilon} = \mathcal{E}_{,\boldsymbol{q}}\delta\boldsymbol{q}. \tag{10}$$

Substituting Eqs. (8) and (10) in Eq. (9) gives

$$\delta\boldsymbol{q}^{\mathrm{T}}\overline{\boldsymbol{M}}\ddot{\boldsymbol{q}} = \delta\boldsymbol{q}^{\mathrm{T}}(\mathcal{F}_{,\boldsymbol{q}}^{\mathrm{T}}(\boldsymbol{f} - \boldsymbol{M}(\mathcal{F}_{,\boldsymbol{qq}}\dot{\boldsymbol{q}})\dot{\boldsymbol{q}}) - \mathcal{E}_{,\boldsymbol{q}}^{\mathrm{T}}\boldsymbol{\sigma}), \tag{11}$$

with

$$\overline{\boldsymbol{M}} = \mathcal{F}_{,\boldsymbol{q}}^{\mathrm{T}}\boldsymbol{M}\mathcal{F}_{,\boldsymbol{q}}. \tag{12}$$

Since the components of the vector $\delta\boldsymbol{q}$ are independent, we obtain the equations of motion

$$\overline{\boldsymbol{M}}\ddot{\boldsymbol{q}} = \mathcal{F}_{,\boldsymbol{q}}^{\mathrm{T}}(\boldsymbol{f} - \boldsymbol{M}(\mathcal{F}_{,\boldsymbol{qq}}\dot{\boldsymbol{q}})\dot{\boldsymbol{q}}) - \mathcal{E}_{,\boldsymbol{q}}^{\mathrm{T}}\boldsymbol{\sigma}. \tag{13}$$

2.3. Linearised equations of motion in a reference configuration

Given the non-linear equations of motion (13), consider now small perturbations around some reference configuration specified by a set of degrees of freedom and its first and second time derivatives $(\boldsymbol{q}_0, \dot{\boldsymbol{q}}_0, \ddot{\boldsymbol{q}}_0)$ such that the actual variables are of the form

$$\boldsymbol{q} = \boldsymbol{q}_0 + \delta\boldsymbol{q}, \quad \dot{\boldsymbol{q}} = \dot{\boldsymbol{q}}_0 + \delta\dot{\boldsymbol{q}}, \quad \ddot{\boldsymbol{q}} = \ddot{\boldsymbol{q}}_0 + \delta\ddot{\boldsymbol{q}}, \tag{14}$$

where the prefix δ denotes a perturbation and should not be confused with the virtual variation operator in Eq. (9). Expanding the equations of motion (13) in their Taylor series expansion and disregarding second and higher order terms yields the linearised equations of motion [13]

$$\overline{\boldsymbol{M}}\delta\ddot{\boldsymbol{q}} + [\overline{\boldsymbol{C}} + \overline{\boldsymbol{D}}]\delta\dot{\boldsymbol{q}} + [\overline{\boldsymbol{K}} + \overline{\boldsymbol{N}} + \overline{\boldsymbol{G}}]\delta\boldsymbol{q} = \mathcal{F}_{,\boldsymbol{q}}^{\mathrm{T}}\delta\boldsymbol{f} - \mathcal{E}_{,\boldsymbol{q}}^{\mathrm{T}}\delta\boldsymbol{\sigma}_a. \tag{15}$$

Here $\overline{\boldsymbol{C}}$ is the velocity sensitivity matrix, $\overline{\boldsymbol{D}}$ is the damping matrix, $\overline{\boldsymbol{K}}$ is the structural stiffness matrix and $\overline{\boldsymbol{N}}$, $\overline{\boldsymbol{G}}$ are the dynamic stiffness and geometric stiffness matrices, respectively. Furthermore, $\delta\boldsymbol{f}$ and $\delta\boldsymbol{\sigma}_a$ represent time-varying perturbations of nodal forces and torques and internal driving forces and torques applied to the multibody system. For the special case when the system is at rest in an equilibrium configuration ($\dot{\boldsymbol{q}}_0 = 0$, $\ddot{\boldsymbol{q}}_0 = 0$, $\delta\boldsymbol{f} = 0$, $\delta\boldsymbol{\sigma}_a = 0$), we can evaluate these matrices as follows:

$$\overline{\boldsymbol{C}} = \boldsymbol{0}, \quad \overline{\boldsymbol{N}} = \boldsymbol{0}, \tag{16a}$$

$$\overline{\boldsymbol{D}} = \mathcal{E}_{,\boldsymbol{q}}^{\mathrm{T}}\boldsymbol{S}_d\mathcal{E}_{,\boldsymbol{q}}, \quad \overline{\boldsymbol{K}} = \mathcal{E}_{,\boldsymbol{q}}^{\mathrm{T}}\boldsymbol{S}\mathcal{E}_{,\boldsymbol{q}}, \tag{16b}$$

$$\overline{\boldsymbol{G}} = -\mathcal{F}_{,\boldsymbol{qq}}^{\mathrm{T}}\boldsymbol{f} + \mathcal{E}_{,\boldsymbol{qq}}^{\mathrm{T}}\boldsymbol{\sigma}, \tag{16c}$$

where $\boldsymbol{S}$, $\boldsymbol{S}_d$ are the stiffness and damping matrices obtained by assembling the element stiffness and damping matrices. For expressions of the matrices in Eqs. (16) when the system is not at rest, the reader is referred to [13].

3. Reduction of degrees of freedom

The equations of motion given by Eq. (13), need to be time-integrated to obtain the time response of the compliant mechanism or flexible manipulator. If high frequency modes are present in the model, explicit time-integrators require small time-steps to provide a stable solution, which reduces their computational efficiency. We will exemplify the cause of these high frequency modes and propose an approach to suppress them.

3.1. Motivation and approach

In Fig. 1, two examples are shown to illustrate the cause of the unwanted higher frequencies. In Fig. 1(a) a simply supported beam is considered where we would like to accurately model the illustrated high frequency bending mode. This requires a minimum of four elements as is shown. However, the model will now also include the generally much higher frequencies of unwanted elongation modes like the one shown in the figure. All elongation

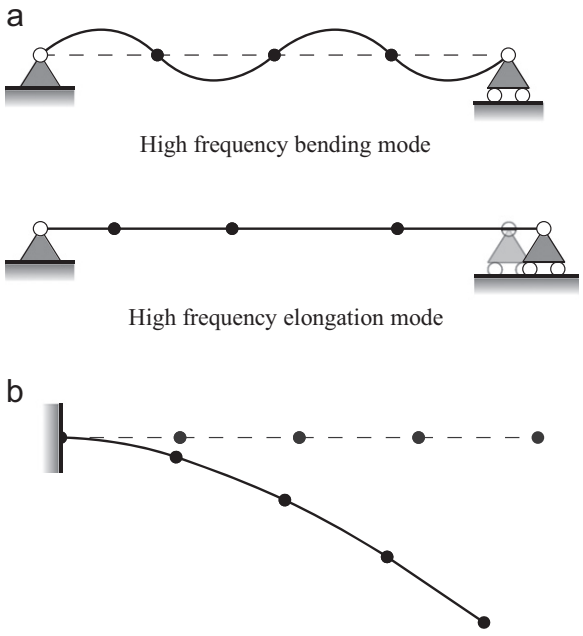

Fig. 1. Examples of models that require multiple finite elements for accurate results: describing high frequency modes of a simply supported beam (a) and large deflections of a clamped beam (b).

modes can be suppressed by prescribing all elongation deformations to be zero, but this is a too strong constraint if e.g. the first elongation mode should be included in the model and only the higher modes should be eliminated. In the second example of Fig. 1(b) a clamped beam is considered that undergoes large deflection. For an accurate representation that captures the geometric non-linear behaviour, one element is not enough as the small deformation assumption would be violated. Therefore, more elements are necessary to ensure small deformations in a co-rotational context, which again introduces high frequency modes.

In both cases, the computational efficiency can be significantly increased if these unwanted high frequency modes are suppressed. For this purpose, constraint relations between the degrees of freedom of the model can be applied. In the case of the simply supported beam, the elongation mode can be suppressed by e.g. relating the elongations of the separate beam elements. In general, the constraint relations can be non-linear, i.e. configuration dependent. In this paper we investigate configuration independent linear constraint relations of the form

$$\boldsymbol{q} = \boldsymbol{V}\boldsymbol{\eta} \quad \text{with } \dim(\boldsymbol{q}) > \dim(\boldsymbol{\eta}), \tag{17}$$

where the columns of the projection matrix $\boldsymbol{V}$ span the allowable motion space with an associated reduced set of coordinates $\boldsymbol{\eta}$. Note that these linear constraints are only applied to the set of deformation coordinates contained in $\boldsymbol{q}$ and that the configuration and deformed state of the mechanism are subsequently determined with the non-linear geometric transfer functions of Eq. (7).

We can write Eq. (11) in terms of the reduced set of coordinates $\boldsymbol{\eta}$, by determining the virtual variations, and the first and second time derivative of Eq. (17) and substituting the resulting expressions, yielding

$$\delta\boldsymbol{\eta}^{\mathrm{T}}\overline{\boldsymbol{M}}_{\eta}\ddot{\boldsymbol{\eta}} = \delta\boldsymbol{\eta}^{\mathrm{T}}[\mathcal{F}_{,\boldsymbol{q}}\boldsymbol{V}]^{\mathrm{T}}(\boldsymbol{f} - \boldsymbol{M}(\mathcal{F}_{,\boldsymbol{qq}}\boldsymbol{V}\dot{\boldsymbol{\eta}})\boldsymbol{V}\dot{\boldsymbol{\eta}}) - \delta\boldsymbol{\eta}^{\mathrm{T}}[\mathcal{E}_{,\boldsymbol{q}}\boldsymbol{V}]^{\mathrm{T}}\boldsymbol{\sigma}, \tag{18a}$$

with

$$\overline{\boldsymbol{M}}_{\eta} = [\mathcal{F}_{,\boldsymbol{q}}\boldsymbol{V}]^{\mathrm{T}}\boldsymbol{M}[\mathcal{F}_{,\boldsymbol{q}}\boldsymbol{V}]. \tag{18b}$$

The components of $\delta\boldsymbol{\eta}$ are now the independent generalised coordinates. Therefore, we obtain for the reduced equations of motion

$$\overline{\boldsymbol{M}}_{\eta}\ddot{\boldsymbol{\eta}} = [\mathcal{F}_{,\boldsymbol{q}}\boldsymbol{V}]^{\mathrm{T}}(\boldsymbol{f} - \boldsymbol{M}(\mathcal{F}_{,\boldsymbol{qq}}\boldsymbol{V}\dot{\boldsymbol{\eta}})\boldsymbol{V}\dot{\boldsymbol{\eta}}) - [\mathcal{E}_{,\boldsymbol{q}}\boldsymbol{V}]^{\mathrm{T}}\boldsymbol{\sigma}. \tag{19}$$

This leaves the determination of the projection matrix $\boldsymbol{V}$. In this paper we propose two approaches: a projection method using a modal basis, and a method where we determine the modeshapes in a variety of configurations after which the dominant contributions are obtained from an analysis using singular value decomposition (SVD).

3.2. Modal basis

For determining a modal basis to suppress the unwanted higher frequency modes, we first partition Eq. (17) as follows:

$$\begin{Bmatrix} \boldsymbol{q}_l \\ \boldsymbol{q}_s \end{Bmatrix} = \begin{bmatrix} \boldsymbol{V}_l & \\ & \boldsymbol{V}_s \end{bmatrix} \begin{Bmatrix} \boldsymbol{\eta}_l \\ \boldsymbol{\eta}_s \end{Bmatrix}, \tag{20}$$

where the subscript l denotes coordinates that can undergo large rotations such as the relative angle of a hinge, and the subscript s denotes coordinates that remain small during simulation such as the deformation coordinates of the beam element. The reason for this partitioning is that usually these deformation coordinates show quite distinct behaviour in relation to a modal analysis. The large rotations in $\boldsymbol{q}_l$ typically result in highly non-linear behaviour that cannot be adequately described by a reduced set of coordinates using a linear projection. Therefore, it is assumed that there is no coupling between the two type of coordinates and modal reduction is only applied to the $\boldsymbol{q}_s$ part. More specifically, the submatrix $\boldsymbol{V}_l$ is chosen to be the identity matrix such that $\boldsymbol{q}_l = \boldsymbol{\eta}_l$. The submatrix $\boldsymbol{V}_s$ is determined by prescribing $\boldsymbol{q}_l = \boldsymbol{0}$ after which the eigenfrequencies and eigenvectors are obtained by solving the eigenvalue problem

$$([\overline{\boldsymbol{K}}_s + \overline{\boldsymbol{G}}_s] - \omega_i^2\overline{\boldsymbol{M}}_s)\boldsymbol{v}_i = \boldsymbol{0}, \tag{21}$$

in the initial configuration for a subset of the linearised equations of motion (15). Here the subscript s indicates the part of the system matrices associated with $\boldsymbol{q}_s$ and ω_i is the ith eigenfrequency with corresponding eigenvector $\boldsymbol{v}_i$ that is collected in the ith column of the submatrix $\boldsymbol{V}_s$. Model order reduction is achieved by omitting the eigenvectors corresponding to unwanted high frequency vibrational modes in $\boldsymbol{V}_s$.

This last step is however not trivial for non-linear systems, where in general the vibrational modes are configuration dependent. This is especially evident in compliant mechanisms that undergo large deflections. To cope with this non-linear behaviour, some of the higher frequency vibrational modes can be kept in $\boldsymbol{V}_s$. Though, choosing which modes to keep is not a trivial task.

3.3. SVD-modal basis

A more systematic approach to determine a projection base that is adequate in the operating range of the mechanism is outlined by the following procedure:

1. In the working range of the mechanism, we determine the linearised equations of motion (15) in n equidistant reference configurations and obtain for each reference configuration a *normalised* modal basis, $\hat{\boldsymbol{V}}_s^{(i)}$. The superscript i refers to the ith reference configuration with $i = 1,2,\ldots,n$.
2. In reference configuration i, we retain the first r modes in $\hat{\boldsymbol{V}}_s^{(i)}$ that should be accurately described.
3 The modes are weighted by their eigenfrequencies as follows:

$$\boldsymbol{Q}^{(i)} = \hat{\boldsymbol{V}}_s^{(i)}\boldsymbol{W}^{(i)}, \tag{22a}$$

with

$$\boldsymbol{W}^{(i)} = \begin{bmatrix} \omega_1^{-a} & & \\ & \ddots & \\ & & \omega_r^{-a} \end{bmatrix}, \tag{22b}$$

where $\boldsymbol{Q}^{(i)}$ is the weighted set of r modes for the ith configuration and a is the weight parameter that scales the weighting. For example for $a=0$ there is no weighting and for $a=1$ the weight on the modes reduces linearly with the eigenfrequency. In fact this parameter can take any real value and is discussed in somewhat more detail in the next section.

4. Concatenate the matrices $\boldsymbol{Q}^{(i)}$ with $i=1,2,\ldots,n$ and form

$$\boldsymbol{Q} = [\boldsymbol{Q}^{(1)}, \boldsymbol{Q}^{(2)}, \ldots, \boldsymbol{Q}^{(n)}]. \tag{23}$$

5. Perform an SVD of the matrix $\boldsymbol{Q}$ and retain the singular vectors with large corresponding singular values to form the projection matrix $\boldsymbol{V}_s$ for the reduction of coordinates as in Eq. (20).

In the first step, the equilibrium reference configurations are chosen to be obtained equidistantly along the direction of motion. This is to ensure that no configuration bias is introduced in the SVD analysis of step 5. Also, to avoid bias, only normalised eigenvectors, or alternatively eigenvectors with the same length, are used in this step.

The weighting by the parameter a in the third step can be used to give higher priority to the lower frequency vibrational modes in the SVD analysis.

4. Examples

Two planar examples are used to demonstrate the proposed approach. A compliant straight guidance example is included to show its effectiveness on the model reduction for compliant mechanisms that undergo large deflections. And as a second example, a flexible manipulator is considered to demonstrate the applicability of the reduction procedure to a more general class of mechanisms. In both examples the equations of motion are numerically integrated with MATLAB's `ode45` integrator, which is an explicit fourth order variable step-size integrator [14].

4.1. Compliant straight guidance

Consider the compliant straight guidance in Fig. 2, which consists of two flexures each modelled with five flexible planar beam elements connected by a rigid intermediate body. Each beam element in the flexures allows for two bending deformations, resulting in a model with 17 degrees of freedom that all remain small in a co-rotational context. The physical properties and dimensions are given in Table 1. The model is excited by a force as function of time

$$f(t) = \begin{cases} \frac{F_{\max}}{2}(1-\cos(20\pi t)), & 0\ \text{s} \le t \le 0.1\ \text{s}, \\ 0, & t > 0.1\ \text{s}, \end{cases} \tag{24}$$

where the maximal applied force is $F_{\max} = 100$ N.

We simulate the time response of the unreduced non-linear model and compute the eigenfrequencies as a function of the x-displacement of the rigid intermediate body. This simulation will serve as a benchmark for the reduced models. In Fig. 3(a), the time response of the x-displacement of the rigid intermediate body is shown. Here the region between the dashed lines indicates the full range of motion of the compliant mechanism.

For the reduced models, we would like to retain the time response of the compliant straight guidance and the second and third eigenfrequencies over the full range of motion. Four reduced

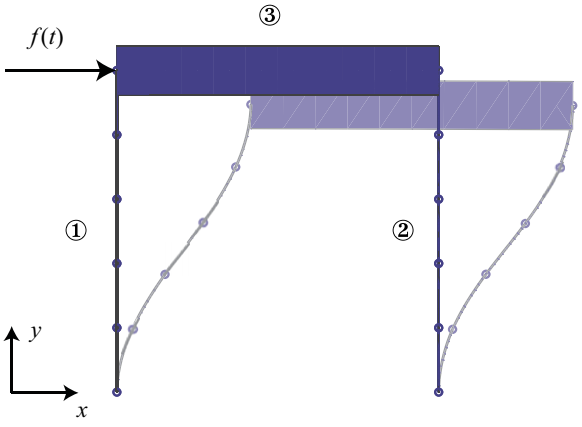

Fig. 2. Two-dimensional straight guidance model. Both flexures are clamped at the bottom end.

Table 1
Physical properties and dimensions of the two-dimensional straight guidance model.

Property	Flexures ① ②	Rigid beam ③
Length, l	0.2 m	0.2 m
Cross-sectional area, A	30×10^{-6} m^2	9×10^{-4} m^2
Cross-sectional area moment of inertia, I	2.5×10^{-12} m^4	6.75×10^{-8} m^4
Young's Modulus, E	2.1×10^{11} N/m^2	
Density, ρ	7600 kg/m^3	7600 kg/m^3

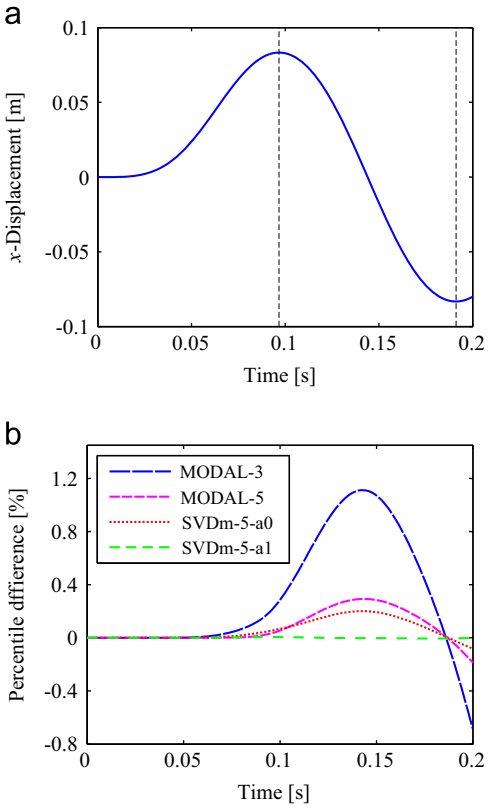

Fig. 3. Time response of the x-displacement of the rigid intermediate body of the unreduced model (a) and the relative time response errors of the reduced models computed with respect to the maximal deflection of 0.0833 m (b).

models are considered. First, using the modal basis as discussed in Section 3.2, a reduced model is created with three time invariant modal modes determined in the initial configuration and is labelled as "MODAL-3". We also consider a reduced model with five time invariant modal modes, labelled as "MODAL-5". The other two reduced models are obtained using the SVD-modal basis approach of Section 3.3. Here we applied an SVD analysis to a set of modes consisting of the first three modes in 10 equidistant reference configurations over the full range of motion. The distinction between the two SVD-modal models is in the weighting parameter of the vibrational modes for the SVD analysis, where we consider a case with no weighting ($a=0$) and a case of linear weighting with the eigenfrequencies ($a=1$). The resulting singular values of both SVD analyses are shown in Fig. 4. The singular values are scaled with the sum of all singular values such that the relative contribution of each singular vector is immediately clear. We retain singular vectors with a contribution larger than 1%. For both weighting cases it appears that five modes are necessary to capture the second and third vibrational modes over the full range of motion. These models are labelled "SVDm-5-a0" and "SVDm-5-a1", respectively, to indicate the number of modes and the weighting. It should be noted that the 1% criterion is used for this example, yet it is not meant to be a general rule.

Fig. 3(b) shows the relative differences between the unreduced and the reduced models of the time response in x-direction of the rigid intermediate body. All four reduced models show good agreement with the unreduced model. The SVD-modal models show better performance than the modal models. For the SVD-modal models, it is clear that by giving higher priority to the lower frequency vibrational modes by setting the weighting parameter $a=1$, the time response error is reduced most. Note that increasing the parameter a too much can give undesirable results for the second and third vibrational modes as all the emphasis in the SVD analysis will be on the first vibrational mode.

In Fig. 5 the second and third eigenfrequencies of the unreduced and reduced models are shown. They are computed over the full range of motion as is indicated by the region between the dashed lines of Fig. 3(a). The MODAL-3 model is able to correctly capture the second and third eigenfrequencies up to a deflection of approximately 0.055 m. After that, due to mode veering of previously higher frequency modes, it is not able to correctly describe the second vibrational mode anymore. This is the reason why the SVD analysis for the SVD-modal models suggested five modes to be used as a reduction basis. From the results of the MODAL-5, SVDm5-a0 and SVDm5-a1 reduced models, it can be concluded that this indeed gives accurate results over the full range of motion. We note that the SVD-modal models are outperforming the MODAL-5 model as they take into account the configuration dependency of the eigenvectors over the full range of motion. Also, we note that a slightly more accurate model is obtained when the eigenvectors are weighted by their eigenfrequencies in the SVD analysis. These results show that the geometric non-linear effects are correctly preserved in the reduced models.

The number of function evaluations required by the explicit variable step-size integrator for the MODAL-3, MODAL-5, SVDm-5-a0 and SVDm-5-a1 is, respectively, 697, 1213, 1411 and 1303. In contrast, the unreduced model required 46,075 function

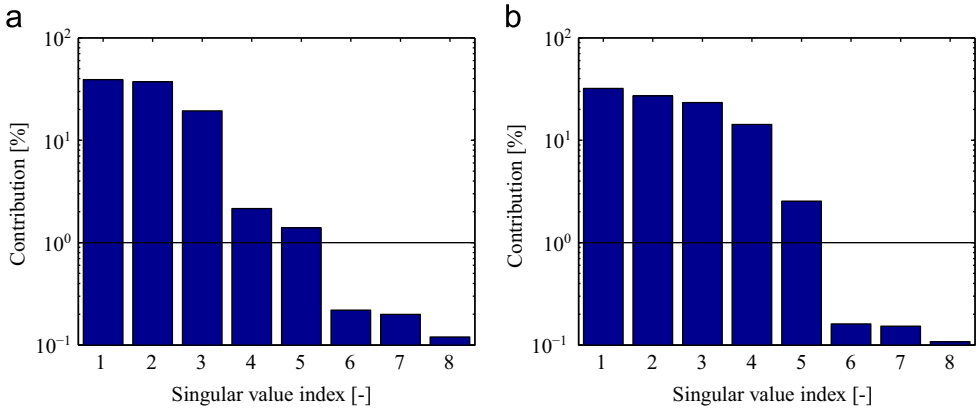

Fig. 4. Singular values scaled with the sum of all singular values, for an SVD analysis using 10 configurations of the straight guidance with no weighting (a) and with weighting a=1 (b).

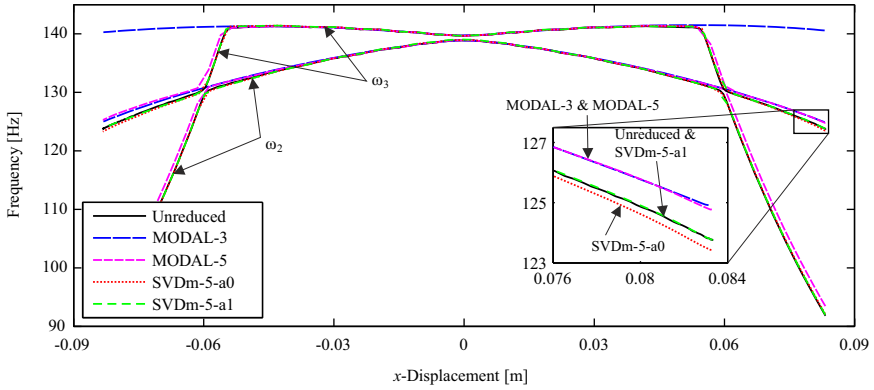

Fig. 5. Second (ω_2) and third (ω_3) eigenfrequencies of the straight guidance as a function of the full range of motion: comparison of the unreduced and reduced models.

evaluations. This illustrates a high increase in computational efficiency for the reduced models.

4.2. Flexible manipulator

Consider the two-link flexible manipulator shown in Fig. 6. This manipulator has been introduced as a benchmark by Schiehlen and Leister [15] and has been quoted in several papers. Some properties are given in Table 2. Different from the original benchmark, we do not include gravity in this paper. Also, instead of prescribing the joint angles with rheonomic constraints, we apply a stiff proportional controller with a gain $k_p = 5\times 10^3$ Nm/rad, in each of the joints. The reference for the controllers are the joint angles $\phi_1(t)$ and $\phi_2(t)$ that are defined by third order functions of time

$$\phi_1(t) = -\phi_2(t) = \begin{cases} \pi/4(-1+72t^3), & 0\ \text{s} \le t < 1/6\ \text{s}, \\ \pi/4(-18t+108t^2-144t^3), & 1/6\ \text{s} \le t < 1/3\ \text{s}, \\ \pi/4(-8+54t-108t^2+72t^3), & 1/3\ \text{s} \le t < 1/2\ \text{s}, \\ \pi/4, & 1/2\ \text{s} \le t. \end{cases} \tag{25}$$

The motion of this manipulator has been computed with a non-linear model in which four flexible planar beam elements are used for each link. Each beam allows two bending modes yielding a model with eighteen degrees of freedom including the two large rotational degrees of freedom of the hinges. Next a reduced model "MODAL-2" is created using two modal modes determined in the initial configuration. Here the deformation coordinates in the beam elements are only reduced as they belong to the category of coordinates $\boldsymbol{q}_s$ from Eq. (20). The degrees of freedom $\boldsymbol{q}_l$ are both joint rotations that are not included in the modal analysis as outlined in Section 3.2. From the results in Fig. 7 it is clear that the reduced model with only four degrees of freedom is able to accurately predict the tip response and the first and second eigenfrequencies. The computational time is significantly reduced, as the reduced model required only 5113 function evaluations for the simulation whereas the unreduced model required 345,145 function evaluations.

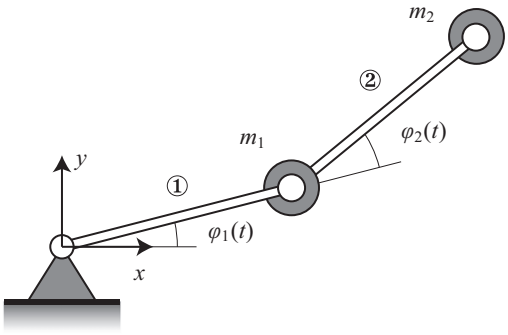

Fig. 6. Planar two-link manipulator model.

Table 2
Physical properties and dimensions of the planar two-link manipulator model (adapted from [15]).

Property	Link ①	Link ②
Length, l	0.545 m	0.675 m
Joint mass, m	1.0 kg	3.0 kg
Cross-sectional area, A	9.0×10^{-4} m^2	4.0×10^{-4} m^2
Cross-sectional area moment of inertia, I	1.69×10^{-8} m^4	3.33×10^{-9} m^4
Young's Modulus, E	7.3×10^{10} N/m^2	7.3×10^{10} N/m^2
Density, ρ	2700 kg/m^3	2700 kg/m^3

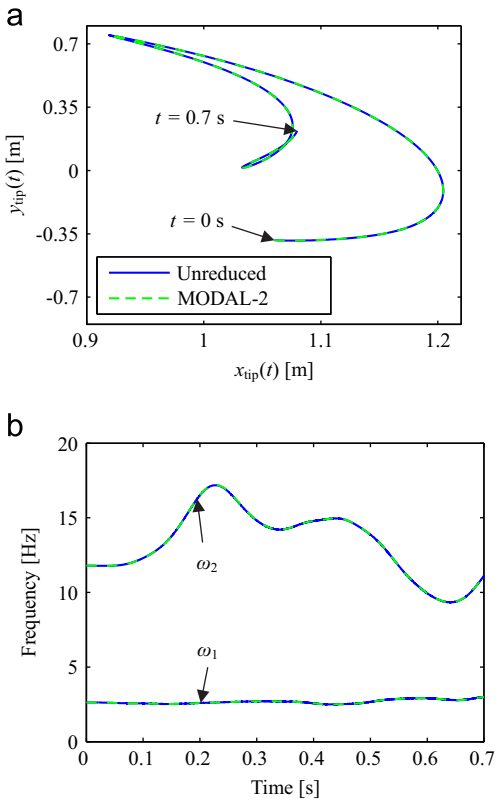

Fig. 7. Motion of the manipulator tip during 0.7 s of simulation (a) and the first (ω_1) and second (ω_2) eigenfrequencies as functions of time (b) for the reduced and unreduced models.

Note that we have not considered the SVD-modal approach in this example. It is thought that in this case only a marginal increase in performance can be obtained as the deflection of the links is already correctly captured using the first two modal modes from the initial configuration. Furthermore, most of the non-linearity arises from varying the hinge coordinates which are not reduced.

5. Conclusions

In this paper a reduction method is proposed for the efficient explicit time-integration of flexible multibody models. For suppressing high frequency modes, linear constraint relations are applied to the independent coordinates that remain small during simulation. Geometric non-linear effects are retained by the geometric transfer functions that describe the configuration of the mechanism in terms of the independent coordinates. The approach is demonstrated by two planar examples: a compliant straight guidance that undergoes large deflection and a flexible manipulator. In both examples it is observed that significant changes in eigenfrequencies during simulation are correctly described by the reduced models. In the case of the compliant straight guidance, mode veering of high frequency modes occurs for rather large deflections. To maintain accuracy for these large deflections, an SVD-modal basis is applied that is derived from an SVD analysis of normalised eigenmodes in a variety of configurations. It is shown that by weighting the eigenmodes with their eigenfrequencies in the SVD analysis, more accurate results are obtained than when no weighting is applied. A significant increase in computational efficiency is observed for the time-

integration of the reduced equations of motion. It should be noted that the reduction methods outlined in this paper appeared to be adequate for the presented planar flexible multibody systems. For other classes of systems like spatial compliant systems somewhat different approaches may be more successful [9].

Acknowledgements

This research is financially supported by the Dutch association Point-One, project MOV-ET PNE08006, of the Dutch Department of Economic Affairs, Agriculture and Innovation.

References

[1] R.G.K.M. Aarts, J. van Dijk, D. Brouwer, J.B. Jonker, Application of flexible multibody modelling for control synthesis in mechatronics, in: ECCOMAS Thematic Conference Multibody Dynamics 2011, Brussels, Belgium.
[2] S.E. Boer, R.G.K.M. Aarts, J.P. Meijaard, D.M. Brouwer, J.B. Jonker, A two-node superelement description for modelling of flexible complex-shaped beam-like components, in: ECCOMAS Thematic Conference Multibody Dynamics 2011, Brussels, Belgium.
[3] A. Cardona, Superelements modelling in flexible multibody dynamics, Multibody System Dynamics 4 (2000) 245–266.
[4] M. Lehner, P. Eberhard, On the use of moment-matching to build reduced order models in flexible multibody dynamics, Multibody System Dynamics 16 (2006) 191–211.
[5] A.A. Shabana, R.A. Wehage, Coordinate reduction technique for dynamic analysis of spatial substructures with large angular rotations, Journal of Structural Mechanics 11 (1983) 401–431.
[6] R.G.K.M. Aarts, J.B. Jonker, Dynamic simulation of planar flexible link manipulators using adaptive modal integration, Multibody System Dynamics 7 (2002) 31–50.
[7] O. Brüls, P. Duysinx, J.-C. Golinval, The global modal parameterization for non-linear model-order reduction in flexible multibody dynamics, International Journal for Numerical Methods in Engineering 69 (2007) 948–977.
[8] J.B. Jonker, J.P. Meijaard, SPACAR—computer program for dynamic analysis of flexible spatial mechanisms and manipulators, in: W. Schiehlen (Ed.), Multibody Systems Handbook, Springer-Verlag, Berlin, 1990, pp. 123–143.
[9] S.E. Boer, R.G.K.M. Aarts, W.B.J. Hakvoort, Model reduction for efficient time-integration of spatial flexible multibody models, Multibody System Dynamics, http://dx.doi.org/10.1007/s11044-013-9346-y, in press.
[10] J.B. Jonker, J.P. Meijaard, Definition of deformation parameters for the beam element and their use in flexible multibody system analysis, in: ECCOMAS Thematic Conference Multibody Dynamics 2009, Warsaw University of Technology, 2009.
[11] W. Visser, J.F. Besseling, Large Displacement Analysis of Beams, Report WTHD-10, Laboratory for Engineering Mechanics, Delft University of Technology, 1969.
[12] J.B. Jonker, A finite element dynamic analysis of spatial mechanisms with flexible links, Computer Methods in Applied Mechanics and Engineering 76 (1989) 17–40.
[13] J.B. Jonker, R.G.K.M. Aarts, J. van Dijk, A linearized input–output representation of flexible multibody systems for control synthesis, Multibody System Dynamics 21 (2009) 99–122.
[14] J. Dormand, P. Prince, A family of embedded Runge–Kutta formulae, Journal of Computational and Applied Mathematics 6 (1980) 19–26.
[15] W. Schiehlen, G. Leister, Benchmark-Beispiele des DFG-Schwerpunkt programmes Dynamik von Mehrkörpersystemen, Zwishenbericht ZB-64, Universität Stuttgart, Institut B für Mechanik, 1991.